

ORIGINAL ARTICLE

Gene amplification-driven RNA methyltransferase KIAA1429 promotes tumorigenesis by regulating BTG2 via m6A-YTHDF2-dependent in lung adenocarcinoma

Chang Zhang^{1,2} | Qi Sun² | Xu Zhang² | Na Qin² | Zhening Pu³ | Yayun Gu^{2,4} | Caiwang Yan^{2,4} | Meng Zhu^{2,4} | Juncheng Dai^{2,4} | Cheng Wang^{2,4,5} | Ni Li⁶ | Guangfu Jin^{2,4} | Hongxia Ma^{2,4} | Zhibin Hu^{2,4,7} | Erbao Zhang^{2,4} | Fengwei Tan⁶ | Hongbing Shen^{1,2,4,7,8}

¹Department of Epidemiology, School of Public Health, Southeast University, Nanjing, Jiangsu 210009, P. R. China

²Department of Epidemiology, Center for Global Health, School of Public Health, Nanjing Medical University, Nanjing, Jiangsu 211166, P. R. China

³Center of Clinical Research, Wuxi People's Hospital of Nanjing Medical University, Wuxi, Jiangsu 214023, P. R. China

⁴Jiangsu Key Lab of Cancer Biomarkers, Prevention and Treatment, Collaborative Innovation Center for Cancer Personalized Medicine, Nanjing Medical University, Nanjing, Jiangsu 211166, P. R. China

⁵Department of Bioinformatics, School of Biomedical Engineering and Informatics, Nanjing Medical University, Nanjing, Jiangsu 211166, P. R. China

⁶Department of Thoracic Surgery, National Cancer Center/National Clinical Research Center for Cancer/Cancer Hospital, Chinese Academy of Medical Sciences and Peking Union Medical College, Beijing 100021, P. R. China

⁷Gusu School, Nanjing Medical University, Nanjing, Jiangsu 211166, P. R. China

⁸Research Unit of Prospective Cohort of Cardiovascular Diseases and Cancers, Chinese Academy of Medical Sciences, Beijing 100142, P. R. China

Correspondence

Hongbing Shen, Department of Epidemiology, School of Public Health, Southeast University, Nanjing, Jiangsu, 210009, P. R. China.
Email: hbshen@njmu.edu.cn

Abstract

Background: Epigenetic alterations have been shown to contribute immensely to human carcinogenesis. Dynamic and reversible N6-methyladenosine (m6A)

Abbreviations: 3'UTR, 3'untranslated region; ANOVA, Analysis of Variance; BSA, bovine serum albumin; cDNA, complementary DNA; CNVs, copy number variations; DAPI, 4',6-diamidino-2-phenylindole; DAVID, Database for Annotation, Visualization, and Integrated Discovery; DEGs, differentially expressed gene; DMEM, Dulbecco's modified Eagle's medium; EDTA, Ethylene Diamine Tetraacetic Acid; EdU, 5-ethynyl-2'-deoxyuridine; EGFR, epidermal growth factor receptor; ES, Enrichment Score; FBS, fetal bovine serum; FDR, false discovery rate; FITC, fluorescein isothiocyanate; FPKM, fragments per kilobase of exon per million reads mapped; GATK, Genome Analysis Toolkit; GEPIA, Gene Expression Profiling Interactive Analysis; GISTIC, Genomic Identification of Significant Targets in Cancer; GO, Gene Ontology; GSEA, Gene Set Enrichment Analysis; H&E, hematoxylin and eosin; HCC, hepatocellular carcinoma; HRP, Horseradish Peroxidase; IgG, immunoglobulin G; IGV, Integrative Genomics Viewer; IHC, immunohistochemistry; IP, immunoprecipitation; KEGG, Kyoto Encyclopedia of Genes and Genomes; lncRNA, long non-coding RNA; LR, early apoptotic cells; LUAD, lung adenocarcinoma; m5C, 5-methylcytosine; m6A, N6-methyladenosine; MB, methylene blue; MeRIP, methylated RNA immunoprecipitation; MeRIP-qPCR, methylated RNA immunoprecipitation -qPCR; MeRIP-seq, methylated RNA immunoprecipitation sequencing; MTT, 3-[4,5-Dimethylthiazol-2-yl]-2,5-diphenyltetrazolium bromid; NC, negative control.; NJLCC, Nanjing Lung Cancer Cohort; NSCLC, non-small-cell lung cancer; OS, overall survival; PBS, phosphate balanced solution; PMSF, phenylmethanesulfonyl fluoride; PVDF, polyvinylidene difluoride; qRT-PCR, quantitative real-time polymerase chain reaction; RIP, RNA immunoprecipitation; RIPA, Radio-Immunoprecipitation Assay; RPMI, Roswell Park Memorial Institute; siRNA, small interfering RNA; SPSS, Statistical Product and Service Solutions; SSC, Saline-Sodium Citrate; STR, short tandem repeat; TCGA, The Cancer Genome Atlas; TPM, transcripts per million; UR, late apoptotic cells; UV, ultraviolet.

Chang Zhang, Qi Sun and Xu Zhang contributed equally to this work.

This is an open access article under the terms of the [Creative Commons Attribution-NonCommercial-NoDerivs](https://creativecommons.org/licenses/by-nc-nd/4.0/) License, which permits use and distribution in any medium, provided the original work is properly cited, the use is non-commercial and no modifications or adaptations are made.

© 2022 The Authors. *Cancer Communications* published by John Wiley & Sons Australia, Ltd. on behalf of Sun Yat-sen University Cancer Center.

Erbao Zhang, Department of Epidemiology, Center for Global Health, School of Public Health, Nanjing Medical University, 101 Longmian Rd., Nanjing 211166, Jiangsu, P. R. China.
Email: erbaozhang@njmu.edu.cn

Fengwei Tan, Department of Thoracic Surgery, National Cancer Center/National Clinical Research Center for Cancer/Cancer Hospital, Chinese Academy of Medical Sciences and Peking Union Medical College, Beijing 100021, P. R. China.
Email: tanfengwei@cicams.ac.cn

Funding information

Science Fund for Creative Research Groups of the National Natural Science Foundation of China, Grant/Award Number: 81521004; National Natural Science Foundation of China, Grant/Award Numbers: 81922061, 82172992, 81903391, 81702266; Research Unit of Prospective Cohort of Cardiovascular Diseases and Cancers, Chinese Academy of Medical Sciences, Grant/Award Number: 2019RU038; Natural Science Foundation of Jiangsu Province, Grant/Award Numbers: BK20211253, BK20190148; Postgraduate Research & Practice Innovation Program of Jiangsu Province, Grant/Award Number: KYCX18_0195

RNA modification regulates gene expression and cell fate. However, the reasons for activation of KIAA1429 (also known as VIRMA, an RNA methyltransferase) and its underlying mechanism in lung adenocarcinoma (LUAD) remain largely unexplored. In this study, we aimed to clarify the oncogenic role of KIAA1429 in the tumorigenesis of LUAD.

Methods: Whole-genome sequencing and transcriptome sequencing of LUAD data were used to analyze the gene amplification of RNA methyltransferase. The *in vitro* and *in vivo* functions of KIAA1429 were investigated. Transcriptome sequencing, methylated RNA immunoprecipitation sequencing (MeRIP-seq), m6A dot blot assays and RNA immunoprecipitation (RIP) were performed to confirm the modified gene mediated by KIAA1429. RNA stability assays were used to detect the half-life of the target gene.

Results: Copy number amplification drove higher expression of KIAA1429 in LUAD, which was correlated with poor overall survival. Manipulating the expression of KIAA1429 could regulate the proliferation and metastasis of LUAD. Mechanistically, the target genes of KIAA1429-mediated m6A modification were confirmed by transcriptome sequencing and MeRIP-seq assays. We also revealed that KIAA1429 could regulate *BTG2* expression in an m6A-dependent manner. Knockdown of KIAA1429 significantly decreased the m6A levels of *BTG2* mRNA, leading to enhanced YTH m6A RNA binding protein 2 (YTHDF2, the m6A “reader”)-dependent *BTG2* mRNA stability and promoted the expression of *BTG2*; thus, participating in the tumorigenesis of LUAD.

Conclusions: Our data revealed the activation mechanism and important role of KIAA1429 in LUAD tumorigenesis, which may provide a novel view on the targeted molecular therapy of LUAD.

KEYWORDS

BTG2, gene amplification, KIAA1429, LUAD, mRNA stability, N6-methyladenosine, RNA methyltransferase, YTHDF2

1 | BACKGROUND

Non-small-cell lung cancer (NSCLC) is the primary type of lung cancer and is the leading cause of cancer mortality worldwide [1]. LUAD is the most prevalent subtype of NSCLC. Over the past years, its morbidity and mortality rate has increased worldwide because LUAD is mostly diagnosed at a late stage, limiting clinical treatment options [2]. Thus, LUAD diagnosis and treatment remain major challenges, which rely on a better understanding of the tumorigenesis mechanisms of LUAD [3].

Accumulating evidence has revealed that genetic, epigenetic and transcriptomic alterations could participate in the tumorigenesis of LUAD [4–6]. Strikingly, epigenetic regulation may lead to profound gene expression changes to facilitate LUAD formation and development [7]. Traditionally, epigenetic alterations included DNA

methylation and histone modification [8]. Recent studies have shown that RNA modifications, as important epigenetic markers, are involved in regulating many biological processes, including tumorigenesis [9, 10]. For instance, METTL3, as an m6A methyltransferase, could promote the translation of epidermal growth factor receptor (EGFR) and the Hippo pathway effector TAZ in human cancer cells [11]. NSUN2, as an RNA methyltransferase, mediates the 5-methylcytosine (m5C) modification of H19 long non-coding RNA (lncRNA) to promote the occurrence and development of hepatocellular carcinoma (HCC) [12]. At the RNA level, an increasing number of chemical modifications have been discovered. Among them, as a posttranscriptional modification, m6A RNA methylation is the most prevalent chemical modification at the RNA epigenetic level [13–15], which regulates gene expression by influencing transcript stability, splicing, translation

efficiency and cap-independent translation [16]. Generally, the m6A methyltransferase complex deposits m6A modifications on RNAs, forming a protein complex consisting of an RNA methyltransferase (METTL3, METTL14, WTAP, and KIAA1429 [also known as VIRMA], termed “writers”) and recognized by YTH m6A RNA binding proteins 1-3 (YTHDF1, YTHDF2 and YTHDF3, an important part of “readers”) [17, 18]. Recent evidence suggests that m6A modification is associated with cancer proliferation, invasion, and metastasis [11, 19, 20]. “Writers” (RNA methyltransferases), as a key member of m6A-related enzymes, are essential for m6A methylation. Several researchers have found that RNA methyltransferases have dysregulated expressions and play important roles in tumorigenesis [21]. For example, METTL3 is upregulated in human bladder cancer compared to normal tissues and promotes bladder cancer progression via the AFF4/NF- κ B/MYC signaling network [22]. WTAP is highly expressed in HCC tissues and promotes liver cancer development via the HuR-ETS1-p21/p27 axis [23].

Although these studies indicate that RNA methyltransferases could play important roles in tumorigenesis, few have explored the reason for the activation of m6A methyltransferase in tumorigenesis, especially at the genome level, such as copy number variations (CNVs). In this study, we aimed to uncover the activated reason of RNA methyltransferase KIAA1429, and we further investigated its biological function and molecular regulatory mechanism in tumorigenesis of LUAD.

2 | METHODS

2.1 | The copy number variations of m6A methyltransferases

First, based on the whole-genome sequencing data of 55 LUAD patients in the Nanjing Lung Cancer Cohort (NJLCC) database (<https://ega-archive.org/datasets/EGAD00001004071>), the sample genome copy number fragment data were identified and obtained using the Genome Analysis Toolkit (GATK) 4 process. In addition, we also obtained the copy number data of LUAD samples (a total of 511 LUAD samples containing copy number variations information) from The Cancer Genome Atlas (TCGA) database by downloading from <https://gdac.broadinstitute.org/>. Combined with the human reference genome data, Genomic Identification of Significant Targets in Cancer (GISTIC) 2.0 software was used to identify gene copy number variations. GISTIC analysis was performed using the GISTIC 2.0 pipeline (GenePattern, <https://genepattern.broadinstitute.org/>). The correspond-

ing GISTIC score = -2 , ≤ -1 , ≥ 1 , and = 2 represented a gene undergoing homozygous deletion, copy-number loss, copy-number gain, and amplification, respectively [24]. Then, we calculated the copy amplification ratio for each m6A RNA methyltransferase. By combining transcriptome sequencing data obtained from the NJLCC and TCGA databases, we used Spearman rank-sum test to evaluate the association of expression level with the copy number of KIAA1429 in samples. The copy numbers of KIAA1429 in the cells were determined using the threshold cycle values from the respective standard curves.

2.2 | Cell culture

The LUAD cell lines used in this study, including A549, SPCA1, NCI-H1299 and the normal human bronchial epithelial cell line HBE, were purchased from the Cell library of Shanghai Institutes for Biological Sciences, Chinese Academy of Sciences (Shanghai, China). A549 cell line was cultured in Roswell Park Memorial Institute (RPMI) 1640 medium (Thermo Scientific HyClone, Grand Island, NY, USA) supplemented with 10% fetal bovine serum (FBS; Life Technologies, Carlsbad, CA, USA). SPCA1, NCI-H1299 and HBE cell lines were cultured in Dulbecco’s modified Eagle’s medium (DMEM; Thermo Fisher Scientific Gibco, Carlsbad, CA, USA) supplemented with 10% FBS. All cell lines were identified by short tandem repeat (STR) analysis (Biowing, Shanghai, China). The cells were cultured in an incubator (Thermo Scientific, Carlsbad, CA, USA) at a temperature of 37°C and CO₂ concentration of 5%.

2.3 | Transfection

The nucleotide sequences of si-KIAA1429/si-YTHDF2/si-BTG2 are shown in Supplementary Table S1. The negative control small interfering RNA (siRNA) was obtained from Invitrogen (San Francisco, CA, USA). Transfections were performed using the Lipofectamine 2000 Kit (Invitrogen, San Francisco, CA, USA). Typically, the cells were evenly added to 6-well culture plates at a certain concentration and transfected with siRNA on the next day. Lentivirus vectors of KIAA1429 knockdown were obtained from GeneChem (Shanghai, China). LUAD cells were added to 6-well dishes and transfected with KIAA1429 knockdown lentivirus or scramble control. KIAA1429 and BTG2 complementary DNA (cDNA) were synthesized and cloned into the expression vector pcDNA3.1. Following the manufacturer’s instructions, the plasmid was transfected into LUAD cells using the X-tremeGENE™ HP DNA

Transfection Reagent (Roche Applied Science, Indianapolis, IN, USA).

2.4 | RNA isolation and quantitative real-time polymerase chain reaction (qRT-PCR) analyses

TRIzol reagent was used to lyse A549, SPC1, NCI-H1299 and HBE cells and extract RNA. Then, the RNA was reversely transcribed into cDNA using a reverse transcription kit (Takara, Beijing, China). TB Green (Takara, Beijing, China) was used to perform qRT-PCR assays according to the manufacturer's instructions. The results were normalized with GAPDH. The primers used are shown in Supplementary Table S1. Each assay was replicated three times.

2.5 | Cell proliferation assays

A cell viability assay kit was performed using the Cell Proliferation Reagent Kit I (3-[4,5-Dimethylthiazol-2-yl]-2,5-diphenyltetrazolium bromide, MTT) (Roche Applied Science, Indianapolis, IN, USA). The cells were seeded in 96-well plates at 2×10^3 cells/well. After transfection for 24 hours, cell viability was determined every 24 hours following the manufacturer's protocol. Each assay was replicated three times. A 5-ethynyl-2'-deoxyuridine (EdU) cell proliferation detection kit (RIBOBIO, Guangzhou, China) was used to detect the cell proliferation ability. The cells were cultured in 24-well plates at 5×10^3 cells/well. After 48 hours of transfection, 50 mmol/L EdU labeling medium was added and then incubated for 2 hours at 37°C and 5% CO₂. Using 4% paraformaldehyde and 0.5% Triton X-100, the cells were stained with an anti-EdU working solution, and the cell nuclei were labeled with 4',6-diamidino-2-phenylindole (DAPI) (RIBOBIO, Guangzhou, China). The percentage of EdU-positive cells was analyzed using fluorescence microscopy (Carl Zeiss, Jena, Germany). Each assay was replicated three times.

2.6 | Colony formation assays

In the colony formation experiment, 1×10^3 cells/well were added into a 6-well dish and cultured in the medium for approximately two weeks. The cells were first fixed with methanol (Sigma Aldrich, St. Louis, MO, USA) and then stained with 0.1% crystal violet (Beyotime Biotechnology, Shanghai, China) for 15 minutes. The colony-forming ability of the clones was reflected by comparing the number of colonies in each group. Each assay was replicated three times.

2.7 | Wound healing assays

The cells were seeded in 6-well dishes with a culture medium overnight. Before transfection, a 10- μ L sterile plastic tip was used to create a wound line across the surface of each dish. Then, the suspension cells were removed with phosphate balanced solution (PBS) (Thermo Fisher Scientific Gibco, Carlsbad, CA, USA), and a new culture medium was added in a humidified 5% CO₂ incubator at 37°C. Images were taken with a microscope (Olympus, Tokyo, Japan) at 24 hours. Each assay was replicated three times.

2.8 | Cell migration assays

The transfected cells in serum-free medium and the medium with 10% FBS were placed in the upper chamber (Corning, New York, NY, USA) and the lower chamber, respectively. After 24 hours of incubation, the cells that passed through the membrane were fixed and stained with methanol and 0.1% crystal violet and then photographed and counted using an inverted microscope (Olympus, Tokyo, Japan). The experiment included three replicates.

2.9 | Flow cytometric analysis

After two days of transfection, the medium supernatant was first collected into a flow tube (BD Bioscience, East Rutherford, NJ, USA), and the cells were collected by trypsinization (Thermo Fisher Scientific Gibco, Carlsbad, CA, USA). Double staining with fluorescein isothiocyanate (FITC)-Annexin V and propidium iodide was performed using the FITC Annexin V Apoptosis Detection Kit (BD Bioscience, East Rutherford, NJ, USA) based on the manufacturer's instructions. The cells were analyzed with a flow cytometer (FACScan, BD Bioscience, East Rutherford, NJ, USA) equipped with Cell Quest software (BD Bioscience, East Rutherford, NJ, USA). The cells were divided into viable cells, dead cells, early apoptotic cells, and late apoptotic cells. The relative proportion of early apoptotic cells and late apoptosis cells were recorded and compared with the control group. Each assay was replicated three times.

2.10 | Western blot assay and antibodies

The treated cells were lysed using Radio-Immunoprecipitation Assay (RIPA) buffer (Beyotime Biotechnology, Shanghai, China) supplemented with a protease inhibitor cocktail (Roche Applied Science, Indianapolis, IN, USA, dilution ratio, 1:100) and

phenylmethanesulfonyl fluoride (PMSF) (Roche Applied Science, Indianapolis, IN, USA, dilution ratio, 1:1000). A 10% precast gel (SurePAGE™, Nanjing, China, 10 wells) was used to load the lysed protein. The protein was then transferred to polyvinylidene difluoride (PVDF) membranes (Sigma Aldrich, St. Louis, MO, USA), blocked with bovine serum albumin (BSA) (Thermo Scientific, Carlsbad, CA, USA), and incubated overnight with primary antibody. The membrane was washed with wash buffer and probed with a secondary antibody (Beyotime Biotechnology, Shanghai, China). Exposure records and quantification were carried out by a developing instrument (Bio-Rad, Universal Hood II, CA, USA). GAPDH antibody was purchased from Cell Signaling Technology (Danvers, MA, USA) (dilution ratio, 1:1000, 5174S) and used as a control. Anti-KIAA1429 (dilution ratio, 1:1000, ab271136) and anti-BTG2 (dilution ratio, 1:200, ab197362) were purchased from Abcam (Cambridge, UK). Each assay was replicated three times.

2.11 | Transcriptome sequencing

Total RNA was isolated from KIAA1429 knockdown and control A549 cells. The concentration of each sample was measured using a NanoDrop 2000 (Thermo Scientific, Carlsbad, CA, USA). The quality was evaluated by an Agilent 2200 (Agilent, Palo Alto, CA, USA). The sequencing library of each RNA sample was prepared using the Ion Proton Total RNA-Seq Kit version 2 based on a protocol provided by the manufacturer. The corresponding data are listed in Supplementary Table S2. Each assay was replicated three times.

2.12 | Gene ontology (GO) analysis

The Database for Annotation, Visualization, and Integrated Discovery (DAVID) (Version 6.8 Beta) was used to perform the enrichment analysis, an online tool for GO enrichment analysis (<https://david.ncifcrf.gov/>) [25]. The GO biological process terms were selected from the top significantly enriched clusters. Bonferroni-corrected *P*-values were identified as significant when below 0.05.

2.13 | Gene set enrichment analysis (GSEA)

To determine the differentially expressed gene (DEG) response to KIAA1429 knockdown, we used GSEA in the GSEA tool to list particular pathways described in previ-

ously known gene sets. A normalized enrichment score was calculated to compare enrichment analysis results across gene sets [26, 27].

2.14 | RNA m6A dot blot assays

Total RNA was first loaded onto a nitrocellulose membrane (Amersham, GE Healthcare, USA) installed in a BioDot apparatus (Bio-Rad, Hercules, CA, USA) with ice-cold 20×Saline-Sodium Citrate (SSC) buffer (Sigma Aldrich, St. Louis, MO, USA). Then, the membrane was cross-linked using ultraviolet (UV), blocked, incubated with m6A antibody (202003, 1:2000, Synaptic Systems, Goettingen, SN, Germany) overnight at 4°C and subsequently incubated with Horseradish Peroxidase (HRP)-conjugated goat anti-mouse immunoglobulin G (IgG) (Beyotime Biotechnology, Shanghai, China) for 1 hour. Finally, the membrane was visualized by an imaging system (Bio-Rad, Universal Hood II, CA, USA). The membrane was stained with 0.02% methylene blue (MB) (Beyotime Biotechnology, Shanghai, China) in 0.3 mol/L sodium acetate (pH 5.2) (Sigma Aldrich, St. Louis, MO, USA) to ensure the consistency of the baseline between the different groups. Experiments were repeated three times.

2.15 | Methylated RNA immunoprecipitation sequencing (MeRIP-seq)

Total RNA was isolated as before, and purified RNA fragments were isolated using the RiboMinus™ Eukaryote Kit version 2 (Invitrogen, Waltham, MA, USA). The fragmented RNA was sorted into two portions. First, immunomagnetic beads with premixed m6A antibody were added to enrich the mRNA fragments containing m6A methylation. The other was used as a control to construct a conventional transcriptome sequencing library. Library preparation and high-throughput sequencing were performed by the Illumina Nova seq 6000 platform of LC-BIO Biotech (Hangzhou, China). Then, the analysis results of enrichment of m6A peaks and location results were converted into bw files and imported into the Integrative Genomics Viewer (IGV) software (Los Angeles, CA, USA) for visual display. According to the position of RNA modification sites of m6A and total reads number in the bw file, the number of reads obtained from the immunoprecipitation (IP) library and Input library was used to quantify the degree of m6A modification. This data was reflected in the coordinate interval of each modification to form a visual representation in IGV software. Each assay was replicated three times.

2.16 | Methylated RNA immunoprecipitation (MeRIP) assay and qRT-PCR

Total RNA was isolated from stable *KIAA1429* knock-down A549 cells and controls. Chemically fragmented RNA (~100 nt) was incubated with an m6A antibody for immunoprecipitation according to the standard protocol of the Magna MeRIP™ m6A Kit (Merck Millipore, Billerica, MA, USA). Briefly, total RNA was preheated at 94°C for 10 minutes, Ethylene Diamine Tetraacetic Acid (EDTA) (Sigma Aldrich, St. Louis, MO, USA) was immediately added, and 3mol/L sodium acetate (Sigma Aldrich, St. Louis, MO, USA), glycogen (Sigma Aldrich, St. Louis, MO, USA) and 100% ethanol (Sigma Aldrich, St. Louis, MO, USA) were added, and the samples were incubated at -80°C overnight. The next day, magnetic beads were prepared, and the MeRIP reaction mixture was prepared and incubated with m6A antibody at 4°C for 2 hours. The last m6A RNA was eluted with 10 mg of m6A 5'-monophosphate sodium salt (Merck Millipore, Billerica, MA, USA) at 4°C for 1 hour. Enrichment of m6A was analyzed using qRT-PCR. Experiments were repeated three times.

2.17 | Tumor formation assay in mice model

Five-week-old male athymic BALB/c mice were purchased from GemPharmatech (Nanjing, China) and maintained under specific pathogen-free conditions. For the in vivo cell proliferation assay, A549 and SPCA1 cells were stably transfected with sh-Ctrl and sh-KIAA1429 using lentivirus (GeneChem, Shanghai, China). The cells were subcutaneously injected into either side of the posterior flanks of the mouse. The tumor volume was measured every few days ($\text{length} \times \text{width}^2 \times 0.5$). At the end of the experiment, the mice were euthanized, and the tumors were removed, weighed, and then fixed for hematoxylin and eosin (H&E), BTG2 and Ki-67 immunostaining analysis. To observe tumor metastasis in the lungs, treated SPCA1 cells were injected into the mice's tail vein. After 60 days, the mice were euthanized, and the lungs were removed. Images of the lungs were taken for recording and used for H&E immunostaining analysis, and the nodules on the lung were counted. All animal care procedures and experiments were conducted following animal welfare guidelines and based on the "3Rs" principle (reduce, replace, refine). This study was conducted in strict accordance with the Guide for the Care and Use of Laboratory Animals of the National Institutes of Health. Our protocol was approved

by the Committee on the Ethics of Animal Experiments of Nanjing Medical University.

2.18 | RNA stability assays

After siRNA and plasmid transfection of A549 and SPCA1 cells for 24 hours, the cells were treated with 10 $\mu\text{g}/\text{mL}$ actinomycin D (Sigma Aldrich, St. Louis, MO, USA), then collected at 0, 2, and 4 hours after treatment. Total RNA was extracted and detected by qRT-PCR. Each assay was replicated three times.

2.19 | RNA immunoprecipitation (RIP) assays

The RIP experiment was performed using the Magna RIP™ RNA binding protein immunoprecipitation kit (CAT.17-701, Millipore, Billerica, MA, USA), and all operations were performed following the manufacturer's instructions. The antibody against YTHDF2 for the RIP assay was purchased from Proteintech (24744-1-AP, Rosemont, PA, USA). Experiments were repeated three times.

2.20 | Statistical analysis

All statistical analyses were performed using the Statistical Product and Service Solutions (SPSS) 22.0 software (SPSS Inc., Chicago, IL, USA). The statistical significance of differences between experimental groups and controls was assessed by the one-sample t-test, and two-tailed unpaired or paired t-test. One-way Analysis of Variance (ANOVA) followed by post hoc Tukey's test was used to compare multiple groups. Spearman's rank correlation coefficient was used to measure the correlation between two continuous variables. The overall survival (OS), the time from diagnosis to last follow-up or last date known to be still alive, was calculated using the Kaplan-Meier method and log-rank test for comparison. Two-sided *P*-values of 0.05 were selected for statistical significance.

3 | RESULTS

3.1 | Copy number amplification could drive higher expression of KIAA1429 in LUAD

We analyzed the copy number amplification for m6A methyltransferases (METTL3, METTL14, WTAP, and KIAA1429) using whole genome sequencing and

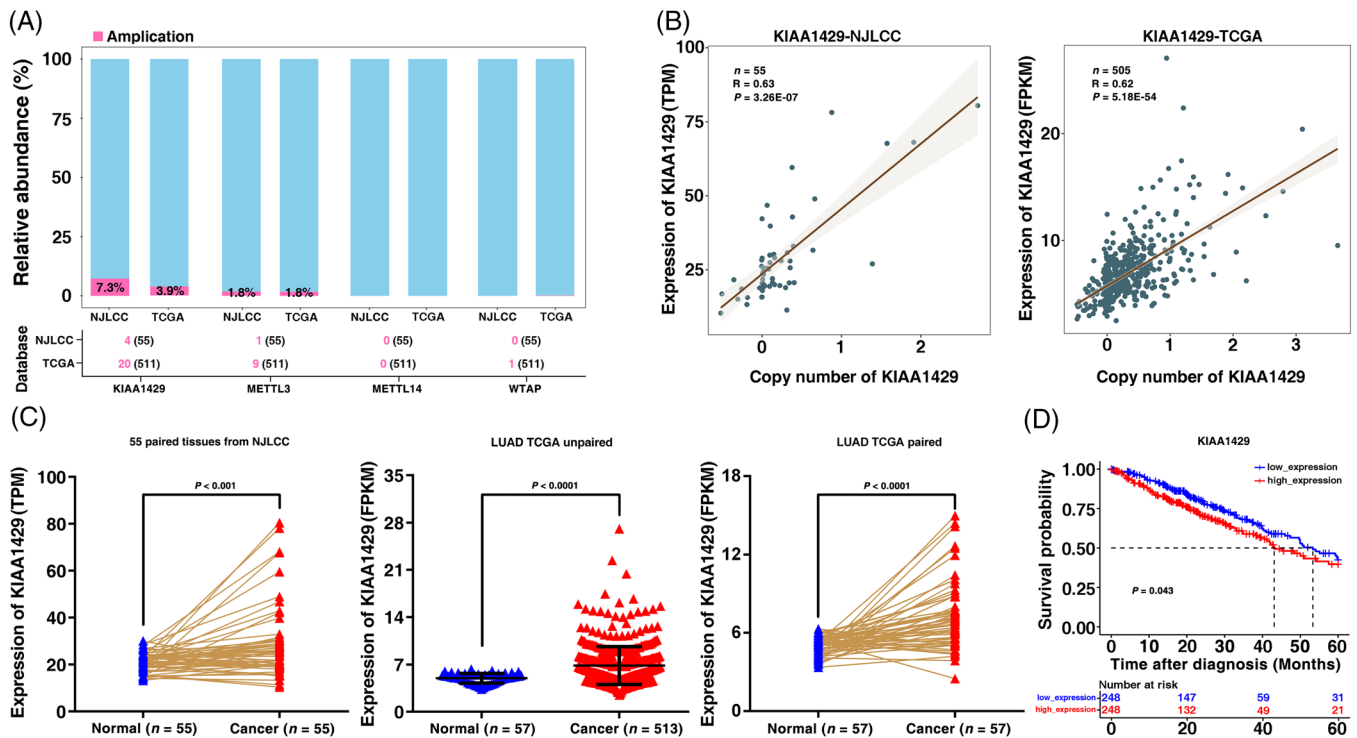


FIGURE 1 High expression of KIAA1429 driven by gene amplification in LUAD. (A) The ratio of copy amplification (the number of copies greater than 1) for KIAA1429, METTL3, METTL14 and WTAP in the NJLCC and TCGA databases. (B) The correlation between the expression of KIAA1429 and its copy number level was analyzed in NJLCC and TCGA LUAD samples. (C) The expression of KIAA1429 in carcinomatous compared with adjacent tissues analyzed using NJLCC paired samples. KIAA1429 expression in LUAD tissues in unpaired (middle panel) and paired (right panel) TCGA data. (D) Using TCGA LUAD data for analysis, we found that high expression of KIAA1429 compared with patients with low levels indicated poor survival (a total of 496 LUAD sample patients with complete prognostic information were analyzed). * $p < 0.05$, ** $P < 0.01$. Abbreviations: LUAD, lung adenocarcinoma; NJLCC, Nanjing Lung Cancer Cohort; TCGA, The Cancer Genome Atlas; TPM, transcripts per million; FPKM, fragments per kilobase of exon per million reads mapped.

transcriptome sequencing of LUAD in the NJLCC ($n = 55$, these cases of the sample having both whole genome sequencing and transcriptome sequencing data) and TCGA database. We observed that KIAA1429 exhibited the highest copy amplification rate in LUAD samples (7.3% in the NJLCC database, 3.9% in the TCGA database) among the four main m6A methyltransferase genes (*METTL3*, *METTL14*, *WTAP*, and *KIAA1429*) (Figure 1A). Although *METTL3* was also amplified in LUAD, the amplification rate was lower than KIAA1429. Many studies have examined the function of *METTL3* in tumorigenesis, including lung cancer [11, 28]. Therefore, we focused on KIAA1429. Additionally, the expression of KIAA1429 was significantly correlated with the copy number level in both the NJLCC LUAD database and TCGA LUAD database (Figure 1B). We also examined the copy number amplification of KIAA1429 in A549, SPCA1, NCI-H1299 and HBE cell lines and found higher copy number of KIAA1429 in these three LUAD cell lines than in HBE (a normal human bronchial epithelial cell line) (Supplementary Figure S1A). Moreover, qRT-PCR analysis showed that the KIAA1429

expression was higher in diverse human LUAD cell lines than in normal human bronchial epithelial cell line (HBE) (Supplementary Figure S1B).

Next, we investigated KIAA1429 expression in 55 LUAD tumor tissues compared with their matched adjacent normal tissues in the NJLCC database. As shown in Figure 1C, the KIAA1429 expression level in cancer tissues was significantly higher than that in the corresponding normal tissues. We further validated this result in the TCGA data of LUAD and revealed that KIAA1429 was also overexpressed in unpaired and paired LUAD tissues (Figure 1C). We also found that high expression of KIAA1429 indicated a poor prognosis in the TCGA dataset (Figure 1D). However, low *METTL3* expression revealed a significantly worse prognosis in LUAD patients (Supplementary Figure S1C). Other methyltransferases, including *METTL14* and *WTAP*, were not statistically significant prognostic factors. The above results indicated that KIAA1429 expression was upregulated in tumor tissues compared with adjacent normal tissues and that high KIAA1429 expression was associated with poor prognosis.

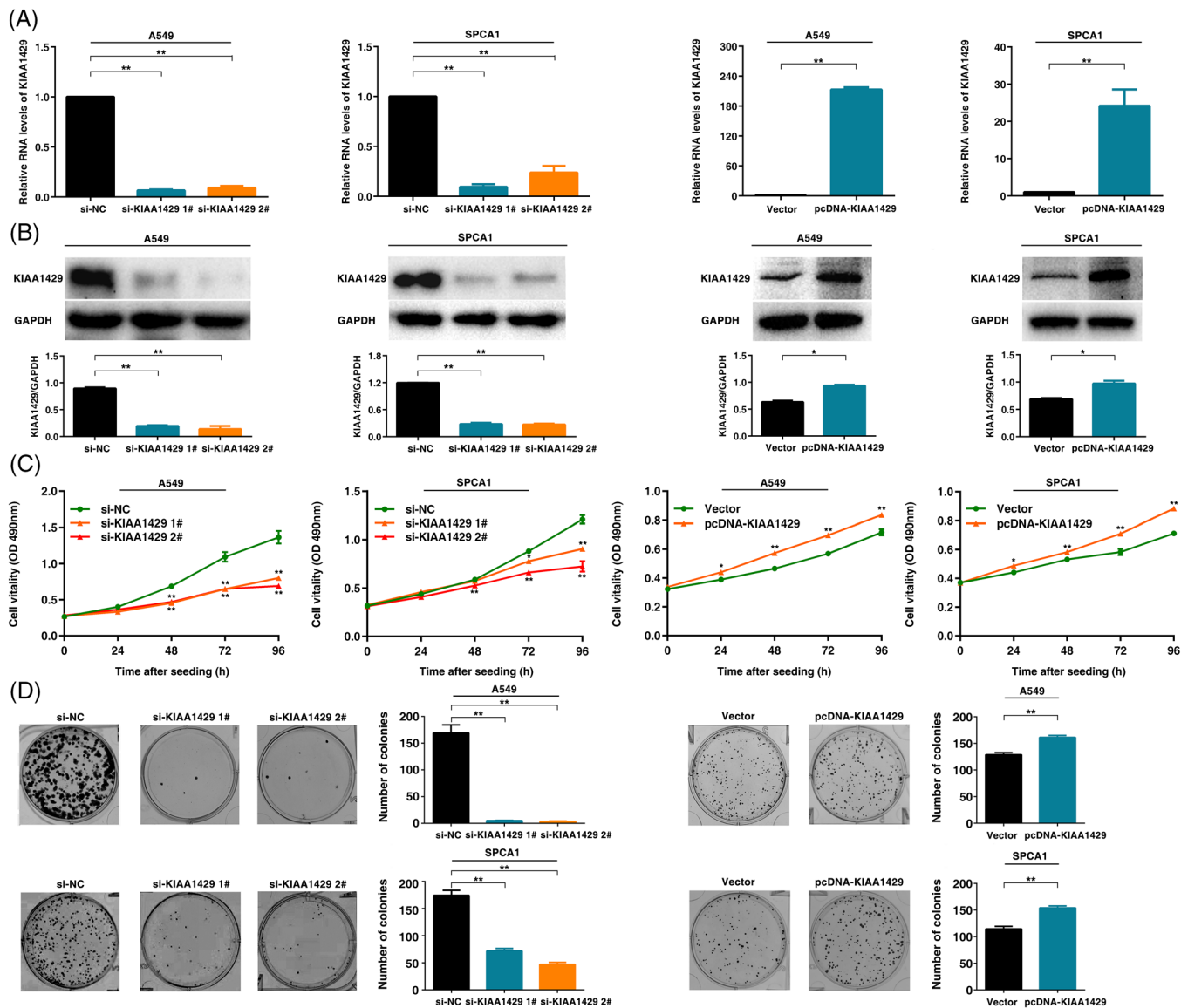


FIGURE 2 KIAA1429 regulates LUAD cell viability and colony formation ability in vitro. (A) *KIAA1429* expression levels were analyzed after transfection of siRNA and overexpression of plasmid compared with the control groups in A549 and SPCA1 cells by qRT-PCR. (B) After transfection with siRNA and plasmid in A549 and SPCA1 cells, the expression of KIAA1429 was detected by Western blotting. (C) MTT assays were used to detect the viability of A549 and SPCA1 cells after KIAA1429 was silenced and overexpressed compared with the control groups. (D) After knocking down KIAA1429 and overexpressing KIAA1429, the colony formation abilities of A549 and SPCA1 cells were detected. Three independent experiments were performed. * $P < 0.05$, ** $P < 0.01$. Abbreviations: LUAD, lung adenocarcinoma; siRNA, small interfering RNA; qRT-PCR, quantitative real-time polymerase chain reaction; MTT, 3-[4,5-Dimethylthiazol-2-yl]-2,5-diphenyltetrazolium bromide.

3.2 | KIAA1429 regulates LUAD cell proliferation and migration in vitro

To explore the biological role of KIAA1429 in LUAD, we used LUAD cell lines (A549, SPCA1 and NCI-H1299). To confirm the function of KIAA1429, we used two independent siRNA-mediated knockdowns and plasmid-mediated overexpression. The mRNA and protein levels confirmed that the expression of KIAA1429 was successfully regulated (Figure 2A, B and Supplementary Figure S2A, B). MTT analysis showed that downregulation of KIAA1429

expression could significantly inhibit cell viability. In contrast, overexpression of KIAA1429 promoted cell proliferation (Figure 2C and Supplementary Figure S2C). Next, colony formation assays showed that the clone formation ability after knocking down KIAA1429 was significantly lower than that of the control group. Furthermore, overexpression of KIAA1429 increased the number of clones (Figure 2D and Supplementary Figure S2D). Transwell assays suggested that cell migration was inhibited after silencing KIAA1429. Overexpressed KIAA1429 promoted cell migration (Figure 3A and Supplementary Figure S2E).

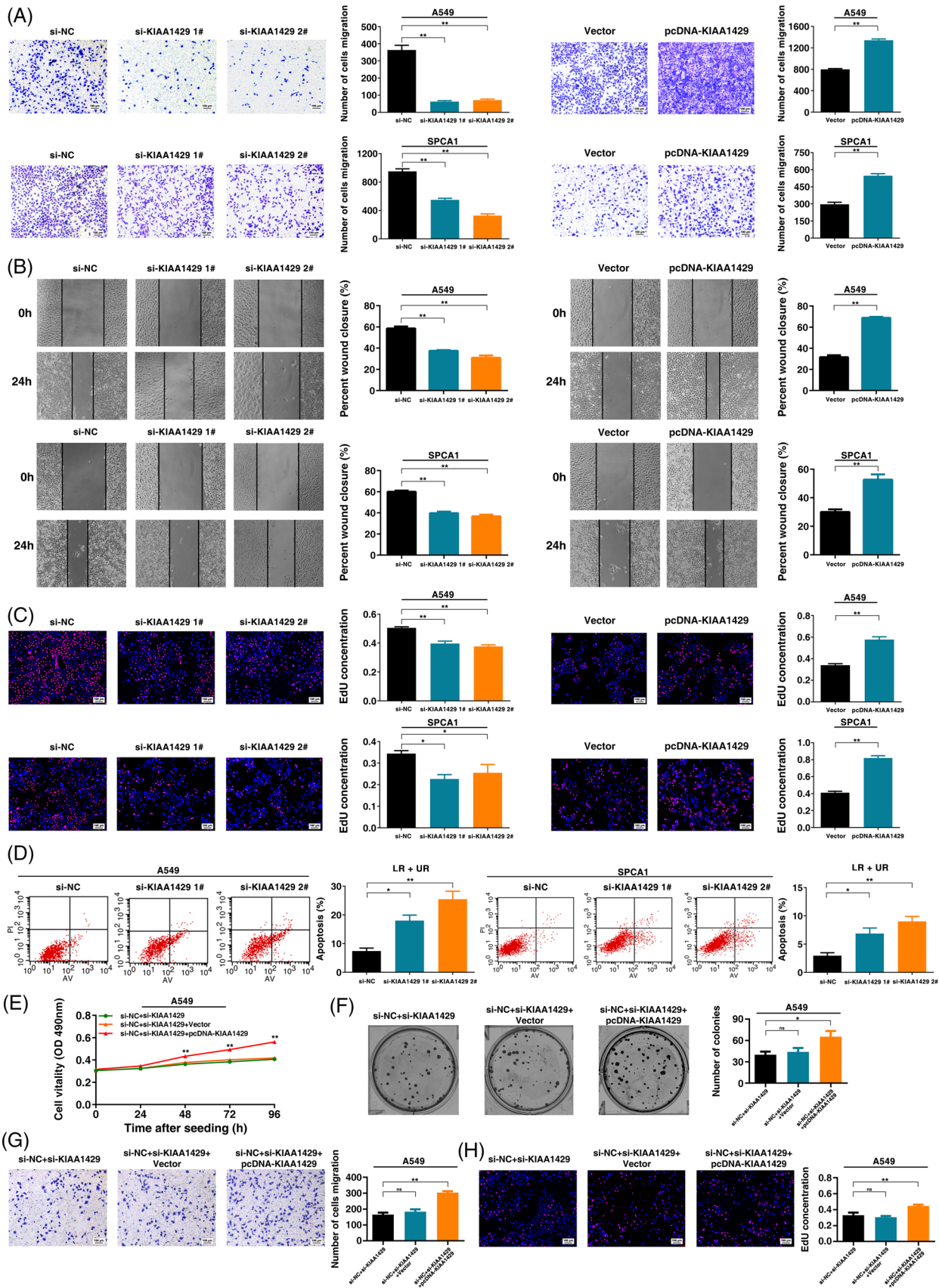


FIGURE 3 KIAA1429 regulates LUAD cell migration, cell proliferation and cell apoptosis in vitro. (A) After transfection with siRNAs and plasmid of KIAA1429, Transwell assays were used to investigate the migratory abilities of A549 and SPCA1 cells. (B) Wound healing assays were used to analyze the migratory activity after transfection with si-KIAA1429 and KIAA1429 plasmids compared with the control

Similarly, compared to control cells, the migratory activity in wound-healing assays was reduced by knockdown of KIAA1429 expression in A549 and SPCA1 cells. Overexpression of KIAA1429 increased migratory activity (Figure 3B). Moreover, the results of the EdU assays demonstrated that KIAA1429 had a significant impact on LUAD cell proliferation (Figure 3C and Supplementary Figure S2F). Flow cytometric analysis found that knockdown of KIAA1429 significantly induced A549, SPCA1 and NCI-H1299 cell apoptosis (Figure 3D and Supplementary Figure S2G). Furthermore, we found that overexpression of KIAA1429 could partly reverse si-KIAA1429-mediated growth and migration suppression (Figure 3E-H). Collectively, the above results indicated that KIAA1429 played an oncogenic role in the tumorigenesis of LUAD.

3.3 | KIAA1429 affected the overall m6A modification level and regulated the mRNA m6A levels of *BTG2* in LUAD

To delineate the functional implications of KIAA1429 and identify its downstream targets in LUAD, we performed RNA transcriptome sequencing to investigate the expression changes in KIAA1429 knockdown cells. In total, we identified 3901 differentially expressed genes (fold change ≥ 1.5), of which 2277 were upregulated and 1624 showed decreased expression in KIAA1429 knockdown A549 cells (Figure 4A and Supplementary Table S2). GO assay was used to explore the underlying pathways mediated by KIAA1429. The results revealed that differentially expressed genes were enriched in gene sets involved in the cell cycle, apoptotic process, cell migration, RNA modification and catabolic process (Figure 4B). Moreover, GSEA revealed that the gene sets were significantly related to the cell cycle and apoptotic processes involved in development (Figure 4C). qRT-PCR assays were performed to verify the changes in several differentially expressed mRNAs involved in growth, apoptosis, oncogenesis pathways and m6A pathway enrichment genes based on the results of RNA sequencing. As shown in Figure 4D, after KIAA1429 knockdown, *BIK*, *BTG2*, *HOXA1*, *EGRI*,

ADAM19 and *KLF4* showed increased expression, while the expression of *PCNA*, *CCND1*, *FAM83A*, and *ATF5* was downregulated in both A549 and SPCA1 cell lines. Importantly, the m6A dot blot assay showed that the overall m6A level decreased after suppressing KIAA1429 expression, indicating that KIAA1429 could affect the overall m6A modification level in A549 cells working as an RNA methyltransferase (Figure 4E). Collectively, our data demonstrated that KIAA1429 might affect downstream target gene expression by regulating m6A modification.

Among the potential targets of KIAA1429, special attention was given to the *BTG2* gene because it was significantly upregulated after the knockdown of KIAA1429. In addition, previous studies have found that as a tumor suppressor, *BTG2* is involved in the tumorigenesis of multiple tumors [29–31]. In addition, the promoter DNA methylation level of *BTG2* could be a stable and reliable biomarker for early-stage lung cancer [32]. Our results indicated that the expression of *BTG2* in LUAD tissues was significantly lower than that of adjacent tissues in the NJLCC database and TCGA database (Figure 5A). We also found that low *BTG2* expression was associated with poor prognosis in the TCGA dataset (Figure 5B). Further research suggested a negative correlation between KIAA1429 and *BTG2* in the NJLCC and TCGA databases (Figure 5C). We found that knockdown of KIAA1429 indeed upregulated *BTG2* expression, while overexpression of KIAA1429 inhibited *BTG2* expression at the RNA and protein levels (Figure 5D, E and Supplementary Figure S3A, B). We found that overexpression of KIAA1429 could partly reverse si-KIAA1429-mediated *BTG2* expression induction (Supplementary Figure S3C). Further results indicated that the knockdown of *BTG2* could reverse KIAA1429 knockdown-mediated *BTG2* induction at both the mRNA and protein levels. In contrast, overexpressed *BTG2* reversed KIAA1429 overexpression-mediated *BTG2* inhibition (Figure 5F, Supplementary Figure S3D-F). Functionally, knockdown of *BTG2* promotes cell proliferation and migration, whereas overexpression of *BTG2* inhibits cell proliferation and migration. In addition, the knockdown of *BTG2* reversed KIAA1429 knockdown-mediated growth and migration inhibition. Overexpressed *BTG2* partly reversed KIAA1429

groups in A549 and SPCA1 cells. (C) The proliferation of A549 and SPCA1 cells was analyzed by EdU after transfection. (D) A549 and SPCA1 cells were stained and analyzed by flow cytometry. (E) MTT assays were used to detect the cell viability after transfection with si-NC+si-KIAA1429, si-NC+si-KIAA1429+vector and si-NC+si-KIAA1429+pcDNA-KIAA1429 in A549 cells. (F) Colony formation assays were used to detect colony formation ability after transfection with si-NC+si-KIAA1429, si-NC+si-KIAA1429+vector and si-NC+si-KIAA1429+pcDNA-KIAA1429 in A549 cells. (G) The migration ability of A549 cells was investigated by Transwell assays after transfection of si-NC+si-KIAA1429, si-NC+si-KIAA1429+vector and si-NC+si-KIAA1429+pcDNA-KIAA1429 in A549 cells. (H) EdU analysis was performed to detect the proliferation of A549 cells after transfection with si-NC+si-KIAA1429, si-NC+si-KIAA1429+vector and si-NC+si-KIAA1429+pcDNA-KIAA1429. Three independent experiments were performed. * $P < 0.05$, ** $P < 0.01$. Abbreviations: LUAD, lung adenocarcinoma; siRNA, small interfering RNA; LR, early apoptotic cells. UR, late apoptotic cells; EdU, 5-ethynyl-2'-deoxyuridine; MTT, 3-[4,5-Dimethylthiazol-2-yl]-2,5-diphenyltetrazolium bromide.

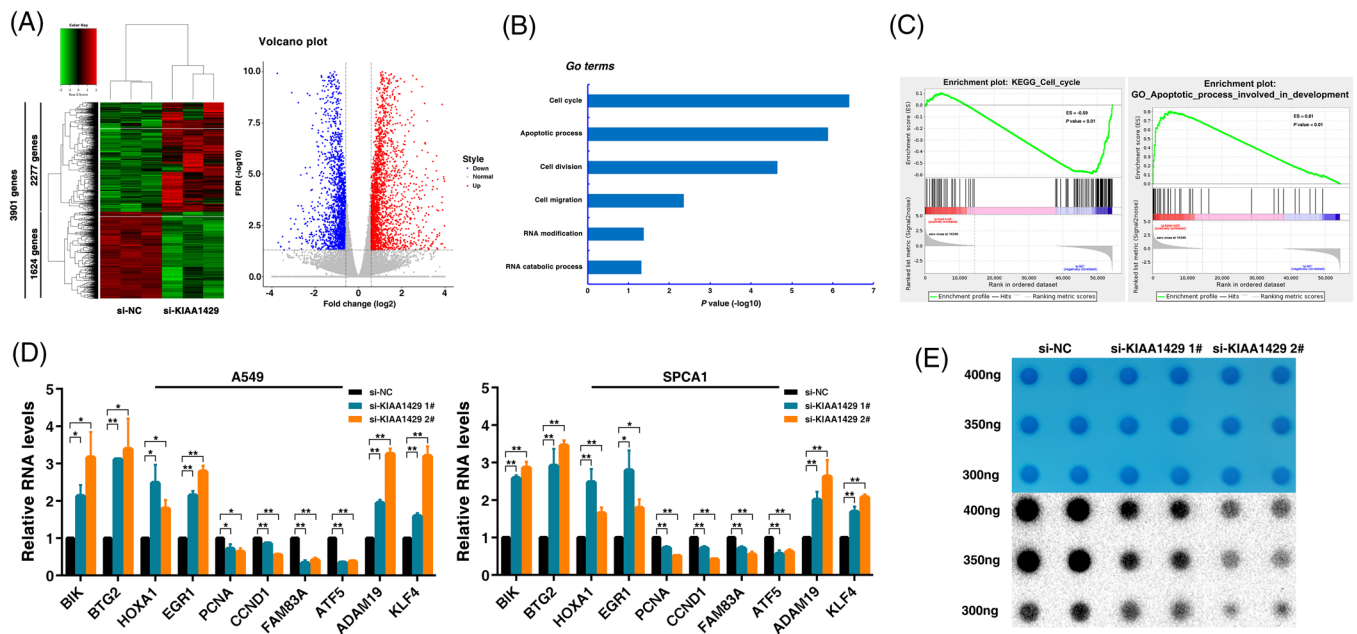


FIGURE 4 The global gene expression profile is regulated by KIAA1429 and potential target genes. (A) Mean-centered, hierarchical clustering of gene transcripts altered (≥ 1.5 -fold change) after knockdown of KIAA1429 in A549 cells with three replicates. Volcano plot depicting up- and downregulated genes identified in response to KIAA1429 knockdown by RNA-seq. (B) GO analysis for all genes with altered expression after knockdown of KIAA1429. (C) GSEA showed that genes in response to KIAA1429 knockdown were enriched for gene sets significantly related to the cell cycle and apoptotic processes involved in development. (D) The altered mRNA levels of genes were selectively confirmed by qRT-PCR in KIAA1429 knockdown cells. (E) The m6A dot blot assay was used to investigate the global m6A abundance after knockdown of KIAA1429 expression compared with the control group in A549 cells. Three independent experiments were performed. * $P < 0.05$, ** $P < 0.01$. Abbreviations: FDR, false discovery rate; GO, Gene ontology; GSEA, Gene Set Enrichment Analysis; KEGG, Kyoto Encyclopedia of Genes and Genomes; ES, Enrichment Score; qRT-PCR, quantitative real-time polymerase chain reaction; m6A, N6-methyladenosine.

overexpression-mediated growth and migration promotion (Figures 5G-I and Supplementary Figure S3G-I). In conclusion, KIAA1429 could regulate the expression of BTG2 to promote tumorigenesis of LUAD.

3.4 | KIAA1429 mediates the expression of BTG2 in an m6A-YTHDF2-dependent manner

Combining the above results, we speculated that KIAA1429 might suppress BTG2 through m6A modification, thus promoting tumorigenesis in LUAD. To further verify the mechanism between KIAA1429 and BTG2, we performed MeRIP-seq assays and found a consistently decreased m6A level in the 3'untranslated region (3'UTR) of BTG2 after KIAA1429 knockdown (Figure 6A). Then, a methylated RNA immunoprecipitation-qPCR (MeRIP-qPCR) assay also verified the reduction in the m6A modification level of BTG2 after KIAA1429 knockdown (Figure 6B). Thus, we confirmed that KIAA1429 regulates the expression of BTG2 in an m6A modification-dependent manner.

Next, we investigated how m6A affected the expression of BTG2. Previous researchers have found that m6A "reader" proteins, including YTHDF1 and YTHDF2, selectively recognize m6A modifications and mediate m6A-containing mRNA degradation, especially YTHDF2, which could lead to mRNA degradation [33]. These results led us to hypothesize that m6A-containing BTG2 mRNA might be recognized and bound by YTHDF2. To test this hypothesis, our analysis found a positive expression correlation between KIAA1429 and YTHDF2 (Figure 6C). To confirm the function of YTHDF2 in LUAD cells, we used siRNA-mediated knockdown of the expression of YTHDF2. MTT analysis showed that YTHDF2 knockdown inhibited A549 cell viability (Supplementary Figure S4A). EdU assays demonstrated that YTHDF2 knockdown inhibited the cell proliferative capacity of A549 (Supplementary Figure S4B). Colony formation assays showed that YTHDF2 knockdown inhibited A549 cell clone formation ability (Supplementary Figure S4C). Next, Transwell assays showed that cell migration was significantly lower after silencing YTHDF2 (Supplementary Figure S4D). To further verify the influence of KIAA1429 and YTHDF2 on the RNA stability of BTG2, we treated A549 and

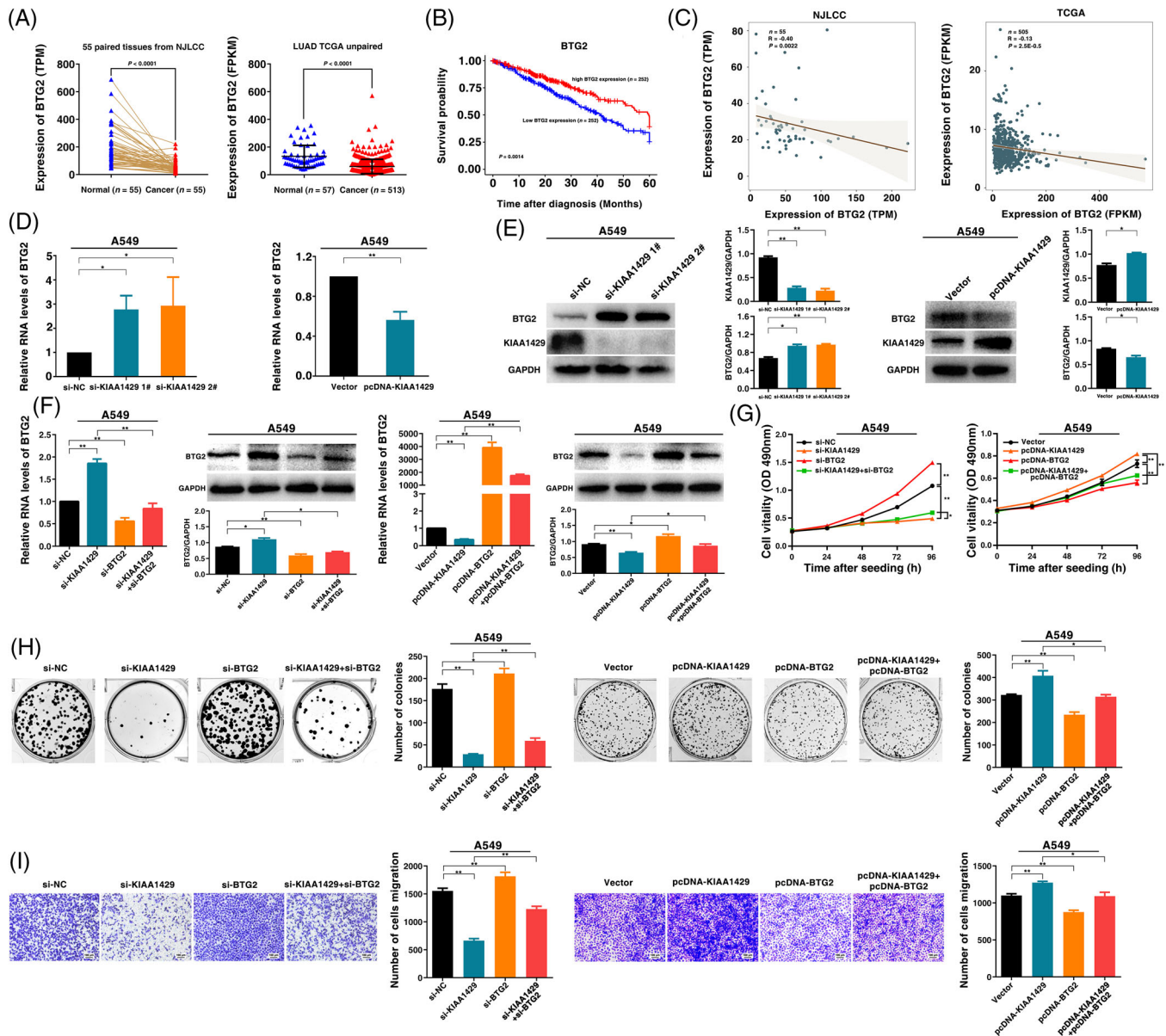


FIGURE 5 KIAA1429 promotes LUAD cell proliferation and migration by inhibiting BTG2 expression. (A) BTG2 expression in 55-paired LUAD tissues was analyzed using the NJLCC database. The expression of BTG2 in TCGA LUAD tissues ($n = 513$) compared with adjacent tissues ($n = 57$) was analyzed with the Gene Expression Profiling Interactive Analysis (GEPIA) online analysis tool (<http://gepia.cancer-pku.cn/>). (B) Low expression of BTG2 indicated poor survival compared with high levels of BTG2 expression according to TCGA LUAD data. (C) Correlation analysis was performed in LUAD tissues from the NJLCC and TCGA databases, and the results indicated a weak negative correlation between KIAA1429 and BTG2. (D) BTG2 mRNA levels were analyzed by qRT-PCR after KIAA1429 knockdown and overexpression compared with the control groups. (E) Western blot assays detected the expression of KIAA1429 and BTG2 after KIAA1429 was silenced and overexpressed compared with the control groups in A549 cells. (F) qRT-PCR assays and Western blot assays detected the mRNA and protein levels of BTG2 in A549 cells after relative treatment. (G) MTT assays were performed to investigate the proliferation of A549 cells after relative treatment. (H) Colony formation assays were detected in A549 cells after relative treatment. (I) Transwell assays were used to determine the migratory abilities of A549 cells after transfection. Three independent experiments were performed. * $P < 0.05$, ** $P < 0.01$. Abbreviations: LUAD, lung adenocarcinoma; NJLCC Nanjing Lung Cancer Cohort; TCGA, The Cancer Genome Atlas; GEPIA, Gene Expression Profiling Interactive Analysis; qRT-PCR, quantitative real-time polymerase chain reaction; MTT, 3-[4,5-Dimethylthiazol-2-yl]-2,5-diphenyltetrazolium bromide.

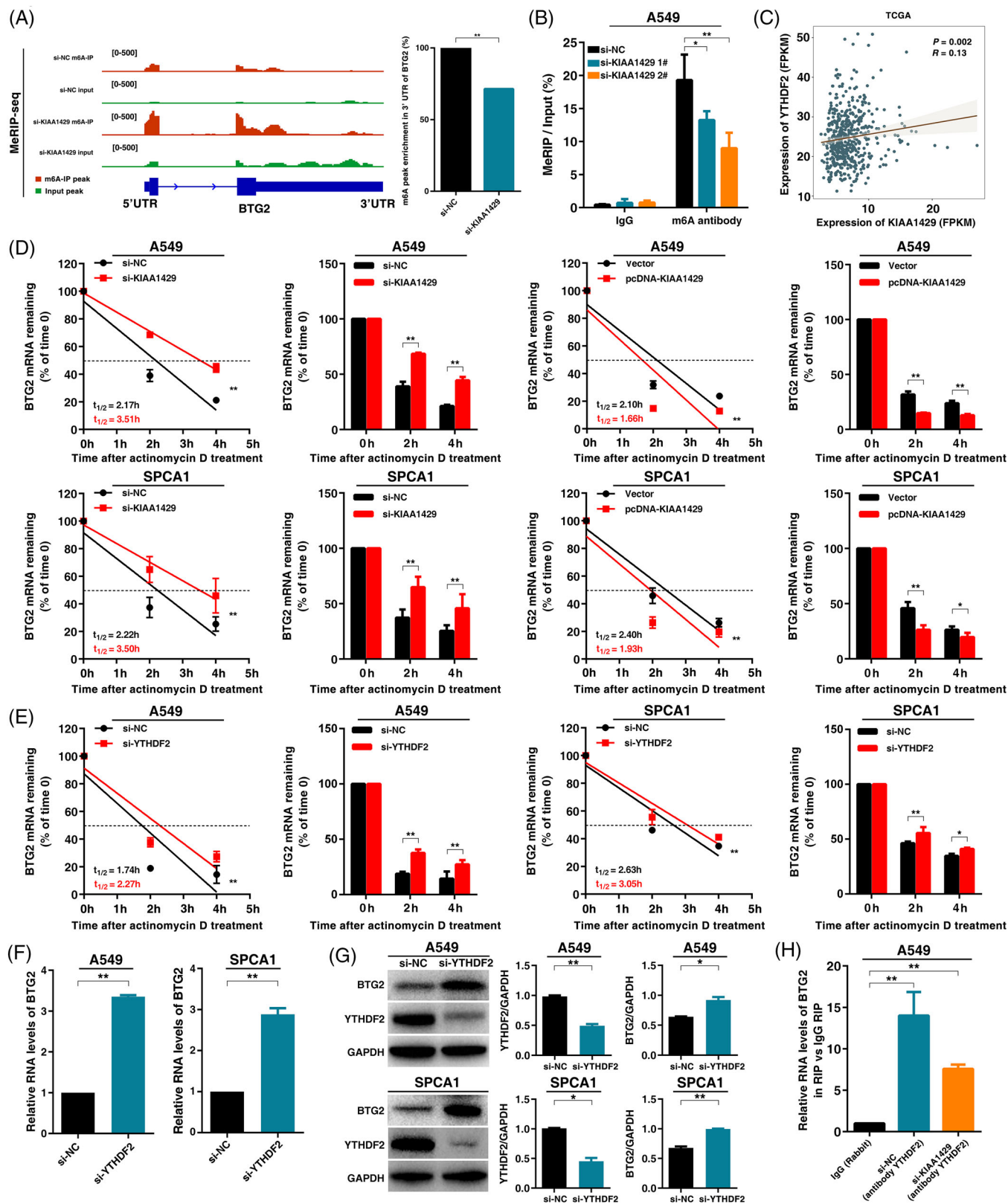


FIGURE 6 KIAA1429 regulates the expression of BTG2 in an m6A-YTHDF2-dependent manner. (A) IGV analysis showed that the m6A peaks among A549 cells were mainly distributed in the 3' UTR. The m6A abundances in *BTG2* transcripts were lower than those in the control group in KIAA1429-knockdown A549 cells. (B) MeRIP-qPCR was performed to quantify the relative m6A modification level of *BTG2* upon KIAA1429 knockdown in A549 cells. (C) Correlation analysis was between the expression of KIAA1429 and YTHDF2 in TCGA LUAD samples. (D) Lifetime *BTG2* mRNA levels in KIAA1429 knockdown and overexpressed cells. (E) Lifetime *BTG2* mRNA levels after silencing YTHDF2 in A549 and SPCA1 cells. (F) and (G) qRT-PCR and Western blot assays were performed to detect *BTG2* levels after knockdown of

SPCA1 cells with the transcription inhibitor actinomycin D after knockdown or overexpression of KIAA1429. Indeed, we found that the knockdown of KIAA1429 increased the half-life of *BTG2* transcripts. In contrast, overexpression of KIAA1429 promoted mRNA degradation of *BTG2* (Figure 6D). The half-life of *BTG2* transcripts was significantly increased after silencing YTHDF2 in both A549 and SPCA1 cells (Figure 6E). These results indicated that the m6A modification of *BTG2* mRNA could be recognized and bound by YTHDF2. qPCR and Western assays showed that *BTG2* mRNA and protein levels were significantly increased after the knockdown of YTHDF2 expression (Figure 6F and G). Moreover, the RIP assay showed that the YTHDF2 protein could directly bind to *BTG2* mRNA. The binding abundance of YTHDF2 on *BTG2* mRNA decreased significantly after silencing KIAA1429 (Figure 6H). Taken together, these results showed that KIAA1429 could regulate *BTG2* in an m6A-YTHDF2-dependent manner in LUAD tumorigenesis.

3.5 | KIAA1429 regulates LUAD cell proliferation and migration in vivo

To further determine whether KIAA1429 affects the proliferation of LUAD cells in vivo, A549 and SPCA1 cell lines stably transfected with sh-KIAA1429 were inoculated into mice using lentivirus. A few days after injection, compared with the control group, the volume of tumors in the sh-KIAA1429 group was significantly reduced (Figure 7A). Moreover, at the end of the experiment, the average tumor weight of the sh-KIAA1429 group was significantly lower than that of the control group (Figure 7A). The positive rate of Ki-67 staining for tumors formed by stable sh-KIAA1429-transfected A549 and SPCA1 cells was significantly lower than that of the control group (Figure 7A). The positive rate of *BTG2* staining was higher in KIAA1429-depleted cells than in the control group (Figure 7A). These findings indicated that knockdown of KIAA1429 inhibited tumor growth in vivo.

To verify the effect of KIAA1429 on cell transfer in vivo, sh-KIAA1429 and a control vector were stably transfected into SPCA1 cells, and the transfected cells were injected into the mice through the tail vein. After 60 days, the metastatic nodules on the lung surface were counted.

Inhibition of KIAA1429 expression reduced the number of metastatic nodules compared with the control group (Figure 7B). The nodules were confirmed by inspecting the entire lungs, slicing the lung, and staining with H&E (Figure 7B). Therefore, the in vivo results supplemented the results of the functional in vitro studies of KIAA1429. In summary, these results suggest that gene amplification-driven KIAA1429 contributes to tumorigenesis of LUAD by regulating *BTG2* in an m6A-YTHDF2-dependent manner (Figure 7C).

4 | Discussion

This study found that KIAA1429 had high copy number amplification in LUAD based on analyses from the NJLCC and TCGA datasets and was associated with poor prognosis in the TCGA dataset. In vitro and in vivo experiments showed that KIAA1429 regulated the cell proliferation and migration, and affected the global m6A modification level of LUAD cells. Moreover, we confirmed that KIAA1429 could affect the expression of *BTG2* by regulating the stability of *BTG2* mRNA in an m6A-YTHDF2 dependent way, thus promoting the tumorigenesis of LUAD.

Prior reports showed that RNA methylation has the same characteristics as epigenetic DNA and histone modifications. Among these modifications, m6A is the most prevalent internal modification in polyadenylated mRNAs [34]. As a “writer” of m6A, RNA methyltransferase is an important factor in aberrant m6A modification. Previous studies noted that RNA methyltransferase was abnormally expressed in various malignant tumors [28, 35]. However, the upstream mechanism of dysregulation has rarely been reported. Our study systematically analyzed the copy number changes of m6A “writers” (KIAA1429, METTL3, METTL14 and WTAP) in LUAD. We found that KIAA1429 and METTL3 had copy amplification in LUAD samples. Although METTL3 was amplified in LUAD, the amplification rate of KIAA1429 was higher than that of METTL3. Many studies have focused on the function of METTL3 in tumorigenesis [18, 28, 35]. As an m6A “writer”, KIAA1429 recruits the catalytic core components METTL3/METTL14/WTAP to guide m6A modification [17, 36]. KIAA1429 mediates preferential mRNA methylation in the 3'UTR and near the stop codon [37]. Previous

YTHDF2 expression in A549 and SPCA1 cells. (H) A RIP experiment for YTHDF2 was performed, and the coprecipitated RNA was subjected to qRT-PCR for *BTG2* after transfection of si-NC and si-KIAA1429. The fold enrichment of *BTG2* in RIP is relative to its matching IgG control RIP. Three independent experiments were performed. * $P < 0.05$, ** $P < 0.01$. Abbreviations: IGV, Integrative Genomics Viewer; IP, immunoprecipitation; m6A, N6-methyladenosine; 3'UTR, 3'untranslated region; MeRIP-qPCR, methylated RNA immunoprecipitation-qPCR; TCGA, The Cancer Genome Atlas; LUAD, lung adenocarcinoma; qRT-PCR, quantitative real-time polymerase chain reaction; RIP, RNA immunoprecipitation; IgG, immunoglobulin G.

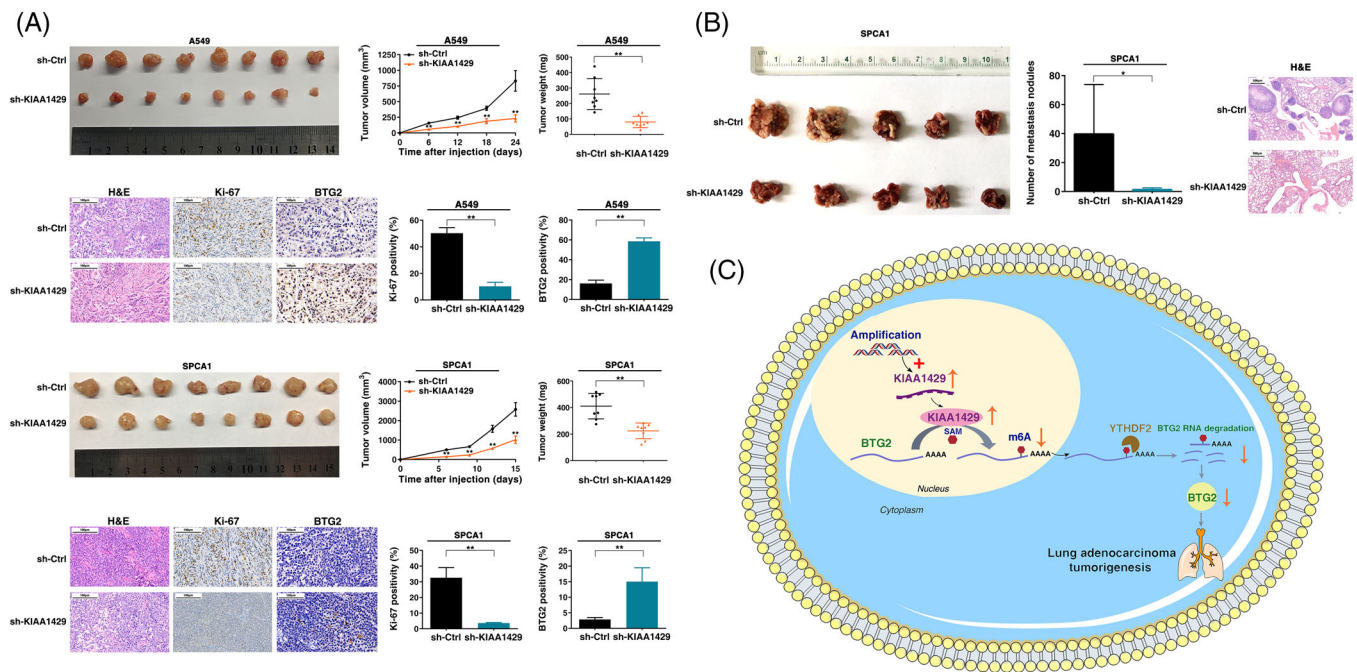


FIGURE 7 KIAA1429 regulates LUAD cell proliferation and migration in vivo. (A) Sh-KIAA1429 was stably transfected into A549 and SPCA1 cells, which were injected into mice. Tumor volumes were calculated after injection every 6 days. Tumor weights were represented as the means of tumor weights \pm S.D. (standard deviation). H&E staining and IHC staining (Ki-67 and BTG2) were performed to detect tumor sections and the expression of BTG2, and it was found that the tumors that developed from the sh-KIAA1429 transfection group were downregulated. (B) SPCA1 cells stably transfected with KIAA1429 knockdown were injected into mice through the tail vein to analyze animal models of tumor metastasis. The number of tumor nodules in the lungs of each group of mice was counted, and entire lung and H&E-stained lung sections were visualized. (C) All the findings in this study were concluded as a schematic diagram. * $P < 0.05$, ** $P < 0.01$. Abbreviations: LUAD, lung adenocarcinoma; H&E, hematoxylin and eosin; IHC, immunohistochemistry.

studies have shown that KIAA1429 could play an essential role in tumorigenesis, including lung cancer [38–40]. For instance, KIAA1429 promotes the migration and invasion of HCC by inhibiting ID2 via upregulating m6A modification of ID2 mRNA [38]. KIAA1429 regulates the expression of MUC3A by modifying m6A, thus regulating the proliferation and migration of LUAD cells [39]. KIAA1429 can accelerate the gefitinib resistance of NSCLC by targeting HOXA1 3'UTR to enhance its mRNA stability [40]. However, the reason for the activation of KIAA1429 remains unclear. Our study first discovered that the activation of KIAA1429 was partly due to copy number amplification in LUAD. These results indicated that genome copy number amplification might be involved in abnormal RNA methylation modification in tumorigenesis. We also found that KIAA1429 was significantly highly expressed in LUAD cells and tissues and that high expression of KIAA1429 was associated with poor prognosis of LUAD patients, which was consistent with the results of previous studies, indicating that the expression level of KIAA1429 could serve as a prognostic marker for LUAD patients [41–43]. We functionally demonstrated the essential role of KIAA1429 in promoting LUAD growth and metastasis via in vitro and in vivo assessments. Further study showed that KIAA1429

transcriptionally regulated a large set of genes linked to cell proliferation and cell migration in LUAD cells, such as *BIK*, *BTG2*, *HOXA1*, *EGRI*, *PCNA*, *CCND1*, *FAM83A* and *ATF5*, and are thus involved in the development of LUAD.

We also demonstrated that KIAA1429 acted as an m6A “writer” to affect the global m6A level in LUAD cells. Then, we conducted RNA-seq in A549 cell lines and found that *BTG2* was a target gene of KIAA1429. *BTG2* is a member of the B cell translocation gene (BTG) family and can regulate cell cycle progression, apoptosis, and differentiation [31]. Several reports have shown that *BTG2* could restrain the cell growth and migration of multiple cancers, including lung cancer [44–46]. Moreover, *BTG2* is one of the p53 target genes involved in the DNA damage repair process in tumor cells [47, 48]. In addition, previous studies have shown that *BTG2* was downregulated in many tumor types, including lung cancer, mainly because it could be modified by DNA methylation in the promoter [48, 49]. However, we found that RNA methylation modification (m6A) could also be an epigenetic marker that inhibits the expression of *BTG2* in LUAD. Here, we identified that the tumor suppressor *BTG2* was significantly downregulated in LUAD tissues and demonstrated a negative correlation with KIAA1429. We also found *BTG2* to be a direct

downstream target of methyltransferase KIAA1429-mediated m6A modification. Taken together, we discovered that the global genes were regulated by KIAA1429, suggesting that KIAA1429 may have a carcinogenic effect on the progression of LUAD. Our results suggested that higher expression of KIAA1429 promotes LUAD tumorigenesis by regulating the expression of critical tumor suppressor genes at the RNA epigenetic level, which added a new layer of epigenetic alteration that contributed to the development of LUAD.

The influences of m6A modification on mRNA are mediated by specific m6A binding proteins, known as m6A “readers” [9]. The YTH domain family protein YTHDF1-3 was identified as an m6A-binding protein in eukaryotic mammals [33, 50]. YTHDF2 recognizes and destabilizes m6A-containing mRNA, and YTHDF1 and YTHDF3 modulate mRNA translation and promote protein synthesis [51]. Because the YTH domain family could play regulatory roles in various biological processes, we hypothesize that m6A-binding proteins might play important roles in the m6A modification mediated by KIAA1429. In our study, we found that the m6A “writer” KIAA1429 and the m6A “reader” YTHDF2 could both modulate *BTG2* expression by regulating its mRNA stability. Therefore, we provided evidence showing that KIAA1429 could mediate the expression of *BTG2* in an m6A-YTHDF2-dependent manner, thereby promoting LUAD tumorigenesis.

5 | CONCLUSIONS

In summary, we revealed that copy number amplification could drive higher expression of RNA methyltransferase KIAA1429 in LUAD, and KIAA1429 could promote the proliferation and metastasis of LUAD cells *in vitro* and *in vivo*. As an RNA methyltransferase gene, *KIAA1429* functions in LUAD by regulating the mRNA of tumor suppressor gene *BTG2* in an m6A-YTHDF2-dependent manner, affecting its mRNA stability, thereby promoting LUAD tumorigenesis. Overall, our study suggests that KIAA1429 played an important role in the tumorigenesis of LUAD and could be regarded as a potential and promising therapeutic target for LUAD.

DECLARATIONS

ACKNOWLEDGMENTS

This work was supported by the Science Fund for Creative Research Groups of the National Natural Science Foundation of China (81521004), the National Natural Science Foundation of China (81922061, 82172992, 81903391, 81702266), the Research Unit of Prospective Cohort of Cardiovascular Diseases and Cancers, Chinese Academy of Medical Sciences (2019RU038), Natural Science Foun-

dation of Jiangsu Province (BK20211253, BK20190148), Postgraduate Research & Practice Innovation Program of Jiangsu Province (KYCX18_0195).

CONFLICT OF INTEREST

The authors declare that they have no competing interests.

AUTHOR CONTRIBUTIONS

CZ, QS and XZ: contributed to designing and organizing the experiments and writing the manuscript. NQ, ZNP, MZ, CW, NL and JCD: contributed to carrying out the data analysis, data analysis. YYG and CWY: contributed to the execution and supervision of experimental operations. GFJ, HXM, ZBH: contributed to design of the work. EBZ, FWT and HBS: contributed to conceiving the ideas, supervising the study, and writing the manuscript. All authors read and approved the final manuscript.

ETHICS APPROVAL AND CONSENT TO PARTICIPATE

The study protocol was approved by the Human Research Ethics Committee of Nanjing Medical University (2017-030), and all of the participants signed an informed consent form. The study protocol was approved by the Committee on the Ethics of Animal Experiments of Nanjing Medical University (IACUC-1812039).

CONSENT FOR PUBLICATION

Not applicable.

DATA AVAILABILITY STATEMENT

The datasets used and/or analyzed during the current study are available from the corresponding author on reasonable request.

REFERENCES

1. Sung H, Ferlay J, Siegel RL, Laversanne M, Soerjomataram I, Jemal A, et al. Global Cancer Statistics 2020: GLOBOCAN Estimates of Incidence and Mortality Worldwide for 36 Cancers in 185 Countries. *CA Cancer J Clin.* 2021;71(3):209–49.
2. Qiu H, Cao S, Xu R. Cancer incidence, mortality, and burden in China: a time-trend analysis and comparison with the United States and United Kingdom based on the global epidemiological data released in 2020. *Cancer Commun (Lond).* 2021;41(10):1037–48.
3. Herbst RS, Morgensztern D, Boshoff C. The biology and management of non-small cell lung cancer. *Nature.* 2018;553(7689):446–54.
4. Garmendia I, Pajares MJ, Hermida-Prado F, Ajona D, Bertolo C, Sainz C, et al. YES1 Drives Lung Cancer Growth and Progression and Predicts Sensitivity to Dasatinib. *Am J Respir Crit Care Med.* 2019;200(7):888–99.
5. Hong S, Gao F, Fu S, Wang Y, Fang W, Huang Y, et al. Concomitant Genetic Alterations With Response to Treatment and Epidermal Growth Factor Receptor Tyrosine Kinase Inhibitors

- in Patients With EGFR-Mutant Advanced Non-Small Cell Lung Cancer. *JAMA Oncol.* 2018;4(5):739–42.
6. Tang WF, Fu R, Liang Y, Lin JS, Qiu ZB, Wu YL, et al. Genomic Evolution of Lung Cancer Metastasis: Current Status and Perspectives. *Cancer Commun (Lond).* 2021;41(12):1252–6.
 7. Topper MJ, Vaz M, Chiappinelli KB, DeStefano Shields CE, Niknafs N, Yen RC, et al. Epigenetic Therapy Ties MYC Depletion to Reversing Immune Evasion and Treating Lung Cancer. *Cell.* 2017;171(6):1284–300.e21.
 8. Bird A. DNA methylation patterns and epigenetic memory. *Genes Dev.* 2002;16(1):6–21.
 9. Fu Y, Dominissini D, Rechavi G, He C. Gene expression regulation mediated through reversible m(6)A RNA methylation. *Nat Rev Genet.* 2014;15(5):293–306.
 10. Berulava T, Buchholz E, Elerdashvili V, Pena T, Islam MR, Lbik D, et al. Changes in m6A RNA methylation contribute to heart failure progression by modulating translation. *Eur J Heart Fail.* 2020;22(1):54–66.
 11. Lin S, Choe J, Du P, Triboulet R, Gregory RI. The m(6)A Methyltransferase METTL3 Promotes Translation in Human Cancer Cells. *Mol Cell.* 2016;62(3):335–45.
 12. Sun Z, Xue S, Zhang M, Xu H, Hu X, Chen S, et al. Aberrant NSUN2-mediated m(5)C modification of H19 lncRNA is associated with poor differentiation of hepatocellular carcinoma. *Oncogene.* 2020;39(45):6906–19.
 13. Desrosiers R, Friderici K, Rottman F. Identification of methylated nucleosides in messenger RNA from Novikoff hepatoma cells. *Proc Natl Acad Sci U S A.* 1974;71(10):3971–5.
 14. Wei CM, Gershowitz A, Moss B. Methylated nucleotides block 5' terminus of HeLa cell messenger RNA. *Cell.* 1975;4(4):379–86.
 15. Roundtree IA, Evans ME, Pan T, He C. Dynamic RNA Modifications in Gene Expression Regulation. *Cell.* 2017;169(7):1187–200.
 16. Roignant JY, Soller M. m(6)A in mRNA: An Ancient Mechanism for Fine-Tuning Gene Expression. *Trends Genet.* 2017;33(6):380–90.
 17. Chen XY, Zhang J, Zhu JS. The role of m(6)A RNA methylation in human cancer. *Mol Cancer.* 2019;18(1):103.
 18. Wang Q, Chen C, Ding Q, Zhao Y, Wang Z, Chen J, et al. METTL3-mediated m(6)A modification of HDGF mRNA promotes gastric cancer progression and has prognostic significance. *Gut.* 2020;69(7):1193–205.
 19. Liu J, Eckert MA, Harada BT, Liu SM, Lu Z, Yu K, et al. m(6)A mRNA methylation regulates AKT activity to promote the proliferation and tumorigenicity of endometrial cancer. *Nat Cell Biol.* 2018;20(9):1074–83.
 20. Ma JZ, Yang F, Zhou CC, Liu F, Yuan JH, Wang F, et al. METTL14 suppresses the metastatic potential of hepatocellular carcinoma by modulating N(6)-methyladenosine-dependent primary MicroRNA processing. *Hepatology.* 2017;65(2):529–43.
 21. Deng X, Su R, Weng H, Huang H, Li Z, Chen J. RNA N(6)-methyladenosine modification in cancers: current status and perspectives. *Cell Res.* 2018;28(5):507–17.
 22. Cheng M, Sheng L, Gao Q, Xiong Q, Zhang H, Wu M, et al. The m(6)A methyltransferase METTL3 promotes bladder cancer progression via AFF4/NF-kappaB/MYC signaling network. *Oncogene.* 2019;38(19):3667–80.
 23. Chen Y, Peng C, Chen J, Chen D, Yang B, He B, et al. WTAP facilitates progression of hepatocellular carcinoma via m6A-HuR-dependent epigenetic silencing of ETS1. *Mol Cancer.* 2019;18(1):127.
 24. Mermel CH, Schumacher SE, Hill B, Meyerson ML, Beroukheim R, Getz G. GISTIC2.0 facilitates sensitive and confident localization of the targets of focal somatic copy-number alteration in human cancers. *Genome Biol.* 2011;12(4):R41.
 25. Huang da W, Sherman BT, Lempicki RA. Systematic and integrative analysis of large gene lists using DAVID bioinformatics resources. *Nat Protoc.* 2009;4(1):44–57.
 26. Pujana MA, Han JD, Starita LM, Stevens KN, Tewari M, Ahn JS, et al. Network modeling links breast cancer susceptibility and centrosome dysfunction. *Nat Genet.* 2007;39(11):1338–49.
 27. Subramanian A, Tamayo P, Mootha VK, Mukherjee S, Ebert BL, Gillette MA, et al. Gene set enrichment analysis: a knowledge-based approach for interpreting genome-wide expression profiles. *Proc Natl Acad Sci U S A.* 2005;102(43):15545–50.
 28. Han J, Wang JZ, Yang X, Yu H, Zhou R, Lu HC, et al. METTL3 promote tumor proliferation of bladder cancer by accelerating pri-miR221/222 maturation in m6A-dependent manner. *Mol Cancer.* 2019;18(1):110.
 29. Shuai Y, Ma Z, Liu W, Yu T, Yan C, Jiang H, et al. TEAD4 modulated LncRNA MNX1-AS1 contributes to gastric cancer progression partly through suppressing BTG2 and activating BCL2. *Mol Cancer.* 2020;19(1):6.
 30. Chen Z, Chen X, Lu B, Gu Y, Chen Q, Lei T, et al. Upregulated LINC01234 promotes non-small-cell lung cancer cell metastasis by activating VAV3 and repressing BTG2 expression. *J Hematol Oncol.* 2020;13(1):7.
 31. Yuniati L, Scheijen B, van der Meer LT, van Leeuwen FN. Tumor suppressors BTG1 and BTG2: Beyond growth control. *J Cell Physiol.* 2019;234(5):5379–89.
 32. Shen S, Zhang R, Guo Y, Loehrer E, Wei Y, Zhu Y, et al. A multi-omic study reveals BTG2 as a reliable prognostic marker for early-stage non-small cell lung cancer. *Mol Oncol.* 2018;12(6):913–24.
 33. Wang X, Lu Z, Gomez A, Hon GC, Yue Y, Han D, et al. N6-methyladenosine-dependent regulation of messenger RNA stability. *Nature.* 2014;505(7481):117–20.
 34. Dominissini D, Moshitch-Moshkovitz S, Schwartz S, Salmon-Divon M, Ungar L, Osenberg S, et al. Topology of the human and mouse m6A RNA methylomes revealed by m6A-seq. *Nature.* 2012;485(7397):201–6.
 35. Deng R, Cheng Y, Ye S, Zhang J, Huang R, Li P, et al. m(6)A methyltransferase METTL3 suppresses colorectal cancer proliferation and migration through p38/ERK pathways. *Onco Targets Ther.* 2019;12:4391–402.
 36. Miao R, Dai CC, Mei L, Xu J, Sun SW, Xing YL, et al. KIAA1429 regulates cell proliferation by targeting c-Jun messenger RNA directly in gastric cancer. *J Cell Physiol.* 2020;235(10):7420–32.
 37. Yue Y, Liu J, Cui X, Cao J, Luo G, Zhang Z, et al. VIRMA mediates preferential m(6)A mRNA methylation in 3'UTR and near stop codon and associates with alternative polyadenylation. *Cell Discov.* 2018;4:10.
 38. Cheng X, Li M, Rao X, Zhang W, Li X, Wang L, et al. KIAA1429 regulates the migration and invasion of hepatocellular carcinoma by altering m6A modification of ID2 mRNA. *Onco Targets Ther.* 2019;12:3421–8.
 39. Zhao W, Xie Y. KIAA1429 promotes the progression of lung adenocarcinoma by regulating the m6A level of MUC3A. *Pathol Res Pract.* 2021;217:153284.
 40. Tang J, Han T, Tong W, Zhao J, Wang W. N(6)-methyladenosine (m(6)A) methyltransferase KIAA1429 accelerates the gefitinib

- resistance of non-small-cell lung cancer. *Cell Death Discov.* 2021;7(1):108.
41. Li F, Wang H, Huang H, Zhang L, Wang D, Wan Y. m6A RNA Methylation Regulators Participate in the Malignant Progression and Have Clinical Prognostic Value in Lung Adenocarcinoma. *Front Genet.* 2020;11:994.
 42. Zhu J, Wang M, Hu D. Deciphering N(6)-Methyladenosine-Related Genes Signature to Predict Survival in Lung Adenocarcinoma. *Biomed Res Int.* 2020;2020:2514230.
 43. Zhuang Z, Chen L, Mao Y, Zheng Q, Li H, Huang Y, et al. Diagnostic, progressive and prognostic performance of m(6)A methylation RNA regulators in lung adenocarcinoma. *Int J Biol Sci.* 2020;16(11):1785–97.
 44. Wei S, Hao C, Li X, Zhao H, Chen J, Zhou Q. Effects of BTG2 on proliferation inhibition and anti-invasion in human lung cancer cells. *Tumour Biol.* 2012;33(4):1223–30.
 45. Zhang YJ, Wei L, Liu M, Li J, Zheng YQ, Gao Y, et al. BTG2 inhibits the proliferation, invasion, and apoptosis of MDA-MB-231 triple-negative breast cancer cells. *Tumour Biol.* 2013;34(3):1605–13.
 46. Takahashi F, Chiba N, Tajima K, Hayashida T, Shimada T, Takahashi M, et al. Breast tumor progression induced by loss of BTG2 expression is inhibited by targeted therapy with the ErbB/HER inhibitor lapatinib. *Oncogene.* 2011;30(27):3084–95.
 47. Tsui KH, Chiang KC, Lin YH, Chang KS, Feng TH, Juang HH. BTG2 is a tumor suppressor gene upregulated by p53 and PTEN in human bladder carcinoma cells. *Cancer Med.* 2018;7(1):184–95.
 48. Choi KS, Kim JY, Lim SK, Choi YW, Kim YH, Kang SY, et al. TIS21(/BTG2/PC3) accelerates the repair of DNA double strand breaks by enhancing Mre11 methylation and blocking damage signal transfer to the Chk2(T68)-p53(S20) pathway. *DNA Repair (Amst).* 2012;11(12):965–75.
 49. Devanand P, Kim SI, Choi YW, Sheen SS, Yim H, Ryu MS, et al. Inhibition of bladder cancer invasion by Sp1-mediated BTG2 expression via inhibition of DNA methyltransferase 1. *FEBS J.* 2014;281(24):5581–601.
 50. Lasman L, Krupalnik V, Viukov S, Mor N, Aguilera-Castrejon A, Schneir D, et al. Context-dependent functional compensation between Ythdf m(6)A reader proteins. *Genes Dev.* 2020;34(19-20):1373–91.
 51. Zaccara S, Jaffrey SR. A Unified Model for the Function of YTHDF Proteins in Regulating m(6)A-Modified mRNA. *Cell.* 2020;181(7):1582–95.e18.

SUPPORTING INFORMATION

Additional supporting information can be found online in the Supporting Information section at the end of this article.

How to cite this article: Zhang C, Sun Q, Zhang X, Qin N, Pu Z, Gu Y, et al. Gene amplification-driven RNA methyltransferase KIAA1429 promotes tumorigenesis by regulating BTG2 via m6A-YTHDF2-dependent in lung adenocarcinoma. *Cancer Commun.* 2022;1–18. <https://doi.org/10.1002/cac2.12325>